# Combretastatin A-4-phosphate effectively increases tumor retention of the therapeutic antibody, $^{131}$I-A5B7, even at doses that are sub-optimal for vascular shut-down

KATHARINE J. LANKESTER[1], ROSS J. MAXWELL[1], R. BARBARA PEDLEY[2], JASON L. DEARLING[2], UZMA A. QURESHI[2], ETHAAR EL-EMIR[2], SALLY A. HILL[1] and GILLIAN M. TOZER[1,3]

[1]Gray Cancer Institute, Mount Vernon Hospital, Rickmansworth Road, Northwood, Middx, HA6 2JR, [2]Cancer Research UK Targeting and Imaging Group, Department of Oncology, Royal Free and University College Medical School Hampstead Campus, UCL, London, NW3 2PF, UK

Received September 7, 2006; Accepted October 30, 2006

**Abstract.** Radioimmunotherapy using $^{131}$I-A5B7, an anti-CEA antibody, in combination with the vascular disrupting agent, combretastatin A4-phosphate (CA-4-P, 200 mg/kg), has produced tumor cures in SW1222 colorectal xenografts. CA-4-P causes acute tumor blood vessel shutdown, which can be monitored in clinical trials using dynamic contrast enhanced magnetic resonance imaging (DCE-MRI). The purpose of this study was to determine the magnitude of the anti-vascular effect of CA-4-P in the SW1222 tumor, at 200 mg/kg and at lower, more clinically relevant doses, using conventional assays; relate effects to changes in DCE-MRI parameters and determine the corresponding effects on tumor retention of $^{131}$I-A5B7. The tumor vascular effects of 30, 100 and 200 mg/kg CA-4-P were determined, at 4- and 24-h post-treatment, using DCE-MRI, uptake of Hoechst 33342 for tumor vascular volume and conventional histology for necrosis. The effect of CA-4-P on tumor and normal tissue $^{131}$I-A5B7 retention was also determined. A significant reduction in tumor DCE-MRI kinetic parameters, the initial area under the contrast agent concentration time curve (IAUGC) and the transfer constant ($K^{trans}$), was demonstrated at 4 h after CA-4-P, for all dose levels. These effects persisted for at least 24 h for the 200 mg/kg group but not for lower doses. A similar pattern was seen for vascular volume and necrosis. Despite this dose response, all three dose levels increased tumor retention of radio labeled antibody to a similar degree. These results demonstrate that moderate tumor blood flow reduction following antibody administration is sufficient to improve tumor antibody retention. This is encouraging for the combination of CA-4-P and $^{131}$I-A5B7 in clinical trials.

*Correspondence to*: Dr Katharine J. Lankester, Sussex Cancer Centre, Royal Sussex County Hospital, Eastern Road, Brighton, BN2 5BE, UK
E-mail: kate.lankester@bsuh.nhs.uk

*Present address:* [3]Cancer Research UK Tumor Microcirculation Group, Academic Unit of Surgical Oncology, University of Sheffield, Floor K, Royal Hallamshire Hospital, Sheffield, S10 2JF, UK

*Key words:* CA-4-P, vascular disrupting agents, radioimmunotherapy, $^{131}$I-A5B7, MRI

## Introduction

In radioimmunotherapy (RIT), a radiolabeled antibody localizes to a tumor-associated antigen, thus targeting radiation directly to a tumor. $^{131}$Iodine [$^{131}$I]-labeled antibodies raised against carcinoembryonic antigen (CEA) have been used for RIT of colorectal carcinoma in the majority of studies (1). However, whereas high response rates and long-term remissions are seen in radiosensitive tumors (such as non-Hodgkin's lymphoma) (2,3), RIT has had only limited success in solid tumors, including colorectal carcinomas (1,4), reflecting their relative radioresistance and the difficulty of obtaining a uniform antibody distribution. Antibody delivery is compromised in poorly-vascularized tumor regions and, even in well-vascularized regions, antibodies may not extravasate efficiently (5,6). Studies investigating the spatial distribution of anti-CEA antibody show that most is retained in the outer regions of tumors (7,8), which tend to be well perfused and where interstitial fluid pressure is low compared with that in central tumor regions (9).

The limited effectiveness of RIT as a single agent in colorectal cancer has led to its investigation in combination with other anti-cancer therapies, such as the vascular disrupting agent, combretastatin A-4-phosphate (CA-4-P). CA-4-P is a tubulin-binding agent that has been shown to depolymerize microtubules of the tubulin cytoskeleton of vascular endothelial cells *in vitro* and to selectively shut down tumor blood flow in animal models *in vivo*, with consequent tumor cell death (10-15). Central hemorrhagic necrosis is observed at 24 h (10,12,16) but a viable peripheral rim of tumor cells persists that can repopulate the tumor centre over the ensuing days (11). Single doses of CA-4-P produce either no or only modest tumor growth delays in animal

models (11,12,17,18), but tumor growth delay is observed in repeated dosing schedules and in combination with cytotoxic agents (11,19,20) or with radiotherapy (11,21-23).

Dynamic contrast-enhanced magnetic resonance imaging (DCE-MRI) of the tissue uptake of gadopentetate dimeglumine (Gd-DTPA) has been used in animal models and in phase I clinical trials of vascular disrupting agents to evaluate the extent and time course of their anti-vascular effect (24-32). The contrast agent diffuses rapidly into the tumor extra-vascular-extracellular space (EES), producing an increase in signal intensity on $T_1$-weighted images. Quantitative parameters relating to tissue blood flow rate, permeability surface-area product and EES may be obtained from modeling of contrast agent kinetics (33,34).

The combination of RIT (using the anti-CEA antibody $^{131}$I-A5B7) and CA-4-P has been tested in SW1222 colorectal xenografts grown in nude mice: 7.4 MBq $^{131}$I-A5B7 was administered followed by 200 mg/kg CA-4-P 48 h later (35). The combination eradicated tumors in 5/6 mice (83%) with no evidence of tumor re-growth when the experiment was terminated >9 months later. When given as a single agent, CA-4-P (200 mg/kg) had no effect on tumor growth, whereas $^{131}$I-A5B7 (7.4 MBq) alone produced significant growth inhibition of about 35 days but no cures. The addition of CA-4-P increased trapping of $^{131}$I-A5B7 in tumors, with an average of 90% more radio-antibody retained at 96 h following $^{131}$I-A5B7 administration compared to controls treated with antibody alone (35).

The combination of $^{131}$I-A5B7 and CA-4-P is thought to be effective as a result of: a) additive cell killing of the tumor centre by CA-4-P and the rim by $^{131}$I-A5B7, and/or b) CA-4-P-induced enhancement of the retention of $^{131}$I-A5B7 in tumor tissue following CA-4-P-induced vessel collapse (35).

A phase I clinical trial of the combination of $^{131}$I-A5B7 and CA-4-P has now started in patients with advanced gastro-intestinal carcinoma. DCE-MRI is being used to measure the acute anti-vascular response (at 4-6 h) to a single dose of CA-4-P. The combination treatment is given a week later ($^{131}$I-A5B7 followed at 48 and 72 h by two further doses of CA-4-P). The DCE-MRI data will be related retrospectively to patient outcome to see if the magnitude of reduction in DCE-MRI kinetic parameters due to CA-4-P can predict response to the combination treatment.

Despite the good effect of the combination in animal studies (35), the dose of CA-4-P used in the published study was double that used in most other pre-clinical studies in mice and there is no information on whether lower doses (which may be more clinically relevant) are effective. Also, there is no information on how CA-4-P dose and DCE-MRI effects relate to antibody retention and therapeutic efficacy. The aims of this pre-clinical study were to use DCE-MRI to determine the dose response and time-course of CA-4-P-induced vascular effects in a model of colorectal cancer (SW1222 human colorectal cancer xenograft - the same model as used in ref. 35) and to relate this information to the dose response for radio-antibody retention. Knowledge of the relationship between DCE-MRI parameter changes and antibody retention will provide a rational basis for interpreting results from the clinical trial, where therapeutic outcome and tumor vascular effects (DCE-MRI) will be measured but where it is not possible to measure antibody retention, and also provide information regarding the magnitude of change in vascular parameters that might be anticipated in the clinical trial.

Specifically, the changes in the quantitative DCE-MRI parameters IAUGC (mM.min) (the initial area under the contrast agent time curve), $K^{trans}$ ($min^{-1}$) (the transfer constant for transport from plasma to tumor EES) in response to CA-4-P were determined. The arterial input function was calculated, as this is required for calculation of $K^{trans}$. The spatial heterogeneity of IAUGC response was also investigated. In addition, histological measures of CA-4-P effect were determined in terms of the functional vascular volume (using Hoechst 33342) and percentage tumor necrosis, for comparison with DCE-MRI results. $^{131}$I-A5B7 retention in tumor and normal tissue was measured following varying doses of CA-4-P, using standard biodistribution techniques.

## Materials and methods

*Mice and tumors*. The human colonic adenocarcinoma cell line SW1222 (36) was maintained in L-15 (Leibovitz) medium (Life Technologies, UK) supplemented with 10% fetal calf serum (Sigma, UK) plus 2 mM glutamine (Life Technologies) and incubated in a humidified incubator at 37˚C in air-5% $CO_2$. Cells ($5x10^6$) were implanted subcutaneously onto the rear dorsum of 4-8-week-old female MF1 nude mice (Harlan UK Ltd., Bicester, UK) anaesthetized with metofane (Methoxy-flurane, Janssen Pharmaceuticals, Ontario, Canada). This CEA-producing xenograft forms well-defined glandular structures around a central lumen, and secretes no measurable CEA into the circulation (37). Animals were selected for treatment after approximately 2-4 weeks when their tumors reached a geometric mean diameter of 6-9 mm for DCE-MRI and antibody biodistribution studies. All animal experiments were performed in full compliance with government regulations and UK Coordinating Committee on Cancer Research (UKCCCR) guidelines on animal welfare and were approved by the local Ethics Review Committee of the Gray Cancer Institute.

*CA-4-P preparation*. CA-4-P was dissolved in 0.9% saline at a concentration of 10 mg/ml.

*DCE-MRI measurements*. Mice were treated with either CA-4-P (Oxigene Inc., Watertown, MA, USA) (at 30, 100 or 200 mg/kg) or 0.9% saline (control) at either 4 or 24 h prior to imaging - making 8 treatment groups in total (6 animals per group). One-hundred mg/kg has been used in other pre-clinical studies (10,12,13) and 30 mg/kg was considered a more clinically relevant dose (see Discussion). Mice were sedated for imaging [0.3 ml/kg hypnorm [fentanyl citrate 0.315 mg/ml and fluanisone 10 mg/ml, Janssen-Cilag, UK], intraperioneally (i.p.), diluted 1:10 with water], restrained in a Perspex jig, then placed in a 6-cm quadrature birdcage coil in a 4.7 Tesla Varian MR system. The temperature inside the magnet was maintained to 35-37˚C using a hot air blower and mouse temperature was monitored continuously via a rectal thermocouple. After initial $T_1$ and $T_2$-weighted images to select a suitable plane through the tumor centre, an inversion

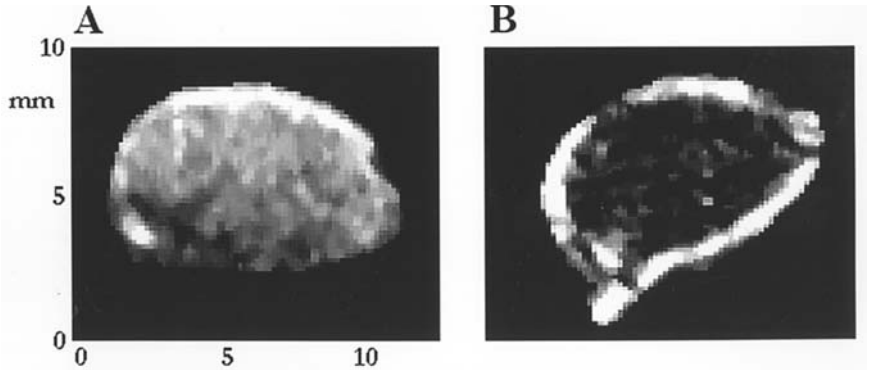


Figure 1. Change in tumor IAUGC following injection of Gd-DTPA at 4 h after treatment with saline (A) or 200 mg/kg CA-4-P (B).

recovery sequence [echo time (TE) 10 msec, repetition time (TR) 2420 msec, inversion times: 100, 400, 800, 1600, 2400 msec) was acquired to calculate pre-contrast tumor $T_1$ values. A gradient echo (dynamic) sequence (TE 2.5 msec, TR 60 msec, flip angle 70˚, field of view 40x45 mm, matrix 256x100 points, in-plane resolution 0.16x0.45 mm, 2 mm slice thickness, time resolution 6 sec, 100 images in total) was then acquired. Gadopentetate dimeglumine (Gd-DTPA, Magnevist®, Schering, UK) was injected as an intravenous (i.v.) bolus at 0.1 mmol/kg (at a concentration of 0.1 mmol/ml, over 5 sec via an infusion pump) during the sixth acquisition.

*DCE-MRI data processing*. Images were processed using Matlab version 5 (The Mathworks, Nantick, MA, USA). A region of interest (ROI) was drawn around the tumor and a section of muscle (as representative normal tissue), using the initial $T_1$-weighted image. Data were analyzed on an individual pixel by pixel basis. The change in signal intensity due to contrast medium accumulation in each pixel was calculated over the imaging period. This was then converted into $T_1$ relaxation time changes using the method described by Hittmair *et al* (38) and the concentration of Gd-DTPA present in each ROI pixel calculated (39). The relaxivity, $r_1$, [the change in relaxation rate per unit of contrast agent concentration (39)] was determined using a set of mouse plasma reference tubes containing Gd-DPTA at varying concentrations and calculated as 4.195 $mM^{-1}.s^{-1}$ at 35˚C [similar to other values quoted at 4.7 Tesla (39,40)]. IAUGC (mM.min) was calculated for the first 90-sec post-contrast (41). A standard compartmental model (42) was used to describe the arterial influx of Gd-DTPA into the tumor EES and its venous efflux. This model was fitted to the dynamic MR concentration data using the method described by Tofts *et al* to obtain values for $K^{trans}$ ($min^{-1}$) (33,34). Data from an *in vivo* and a blood-sampling method of determining arterial input function, Cp, were simultaneously fitted to a bi-exponential function: $Cp = D [a_1e (^{-m}{}_1{}^t) + (a_2e (^{-m}{}_2{}^t)]$ where D is the dose of Gd-DTPA (mmol/kg). The values obtained for the four parameters were: $a_1$=10.19, $a_2$=3.81, $m_1$=4.65, $m_2$=0.09. Parameter values were calculated for each pixel and then median values obtained for the whole ROI. Mean parameter values for each treatment group were then calculated.

To investigate spatial heterogeneity of tumor response to CA-4-P, mean IAUGC values were calculated for three regions, determined by their distance from the edge of the tumor: rim (within 4 pixel layers from the edge, corresponding to a distance of <1 mm); intermediate (5-10 layers from the edge, or 1-3 mm); centre (>10 layers from the edge, or >3 mm).

*Histology*. Tumors used for DCE-MRI imaging at 24-h post-treatment with CA-4-P were scored for necrosis, following staining with haematoxylin and eosin to demonstrate morphology. Using a grid eyepiece graticule marked in 100 squares, each tumor section was assessed at x10 magnification, by scoring each square as undamaged tumor or necrosis. The percentage necrosis was then calculated for each tumor. In a separate experiment, functional vascular volume was determined in control tumors and at 4 or 24 h following treatment with 30, 100 or 200 mg/kg of CA-4-P using Hoechst 33342 (Sigma-Aldrich, Dorset, UK) using the method described previously (43,44).

*Antibody radiolabeling*. The monoclonal anti-CEA IgG antibody A5B7 was labeled with $^{131}I$ using the chloramine T method to a specific activity of 180 MBq/1 mg protein, and sterilized by passing through a 0.22 $\mu$m Gelman filter (Northampton, UK).

*Effect of CA-4-P dose on $^{131}I$-A5B7 biodistribution*. Four groups of four mice bearing the SW1222 xenograft were given 0.9 MBq/5.0 $\mu$g $^{131}I$-labeled A5B7 in 0.1 ml saline i.v. into the tail vein. After 48 h, when the antibody had achieved maximum tumor levels (35), they subsequently received either no further treatment (control group), or a single i.p. dose of CA-4-P (30, 100 or 200 mg/kg). The mice were bled at 96-h post antibody administration (48 h post CA-4-P) and then liver, kidney, lung, spleen, colon, muscle and tumor were removed for comparative activity assessment by $\gamma$-counter (Storm; Pharmacia, Milton Keynes, UK). Results were expressed as percentage injected dose per gram of tissue (% injected dose/g).

*Statistics*. For the DCE-MRI data, a one-way analysis of variance (ANOVA) was performed to look for a significant difference between treatment groups (JMP Statistics, version 3.2.6, SAS Institute, Inc, Cary, USA). If the ANOVA was significant ($p<0.05$), then an appropriate post-test comparison of individual means was performed to look for significant

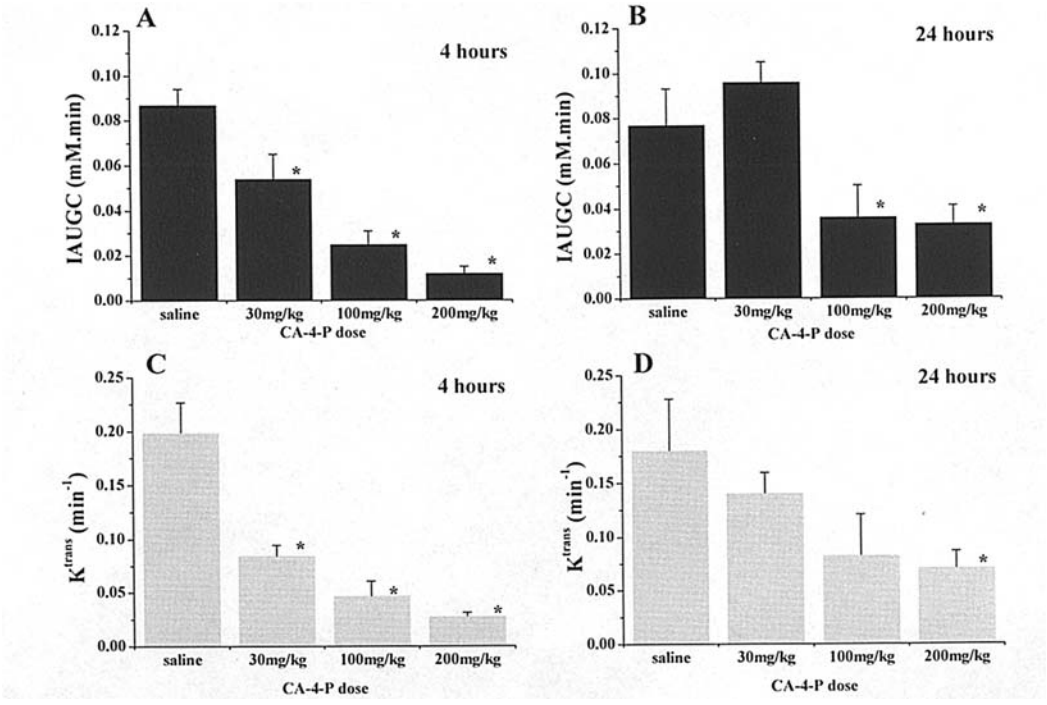


Figure 2. Mean tumor IAUGC and $K^{trans}$ for each treatment group at 4 h (A and C) and 24 h (B and D) respectively. Bars are means of groups of 6 animals ± one standard error of the mean. *Significant vs control ($p<0.05$).

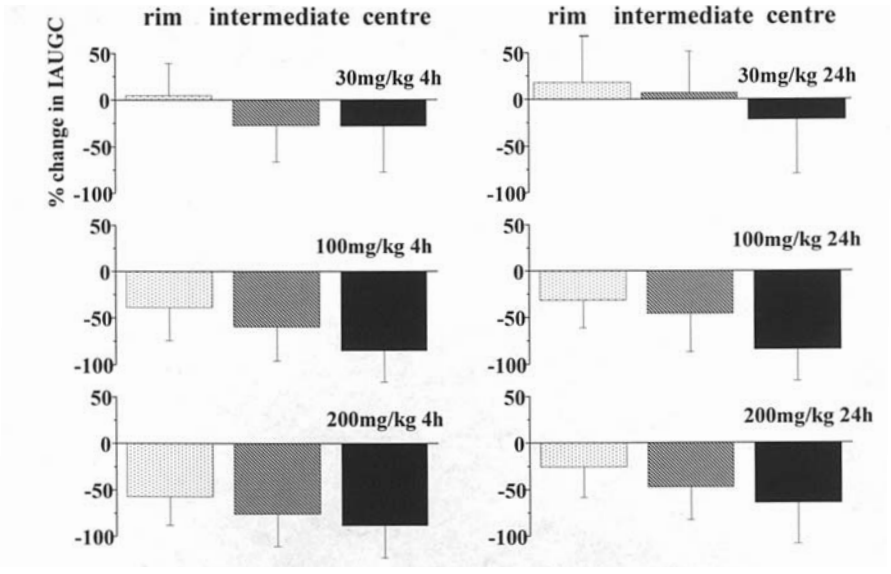


Figure 3. Tumor IAUGC spatial heterogeneity, showing difference in change in IAUGC for tumor rim (white), intermediate zone (grey) and centre (black) for different doses of CA-4-P.

differences between dose levels. Linear regression analysis was used to test for a dose-response relationship. For the antibody biodistribution experiments, different treatment groups were compared using the Mann-Whitney U test. ANOVA was also used for the necrosis and functional vascular volume data.

## Results

*DCE-MRI kinetic parameters*. Fig. 1 shows a representative change in tumor IAUGC at 4 h following administration of saline (Fig. 1A) or 200 mg/kg CA-4-P (Fig. 1B). There was a dose dependent effect at 4 h for both IAUGC and $K^{trans}$ (significant difference between treatment groups on ANOVA, both $p<0.00001$) and at 24 h for IAUGC (ANOVA, $p=0.005$). At 4-h post-treatment, a significant reduction was seen at all dose levels in tumor IAUGC and $K^{trans}$ versus control (Fig. 2A and 2C). At 24-h post-treatment, a significant reduction in tumor IAUGC persisted at 100 and 200 mg/kg and in $K^{trans}$ at 200 mg/kg versus control (Fig. 2B and D). Linear regression analysis was highly significant for a dose-response relationship at 4 h ($r=-0.80$, $p<0.0001$) and significant at 24 h ($r=-0.58$, $p<0.01$) for tumor IAUGC. There was also a significant dose response relationship for tumor $K^{trans}$ at 4 h ($r=-0.72$,

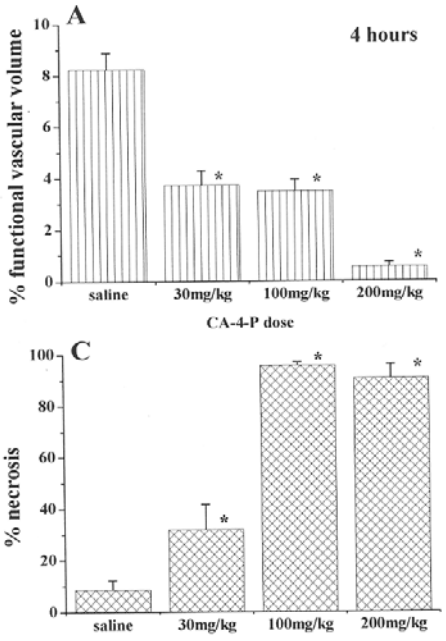


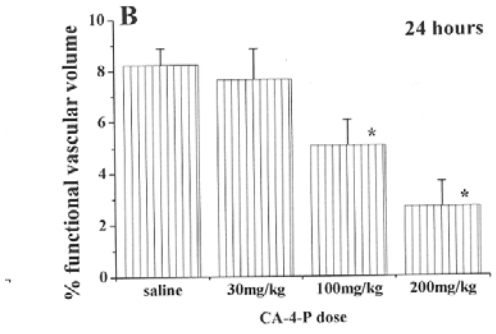


Figure 4. Change in functional vascular volume at 4 h (A) and 24 h (B), and percentage necrosis seen at 24 h (C) following treatment with CA-4-P. Bars are means ± one standard error of the mean. *Significant vs control ($p<0.05$). (A) Number of animals. N =11, 11, 8 and 7 for control, 30, 100 and 200 mg/kg CA-4-P respectively. (B) N =11, 10, 11 and 12 for control, 30, 100 and 200 mg/kg CA-4-P at 24 h respectively. (C) N =6 for each treatment group.

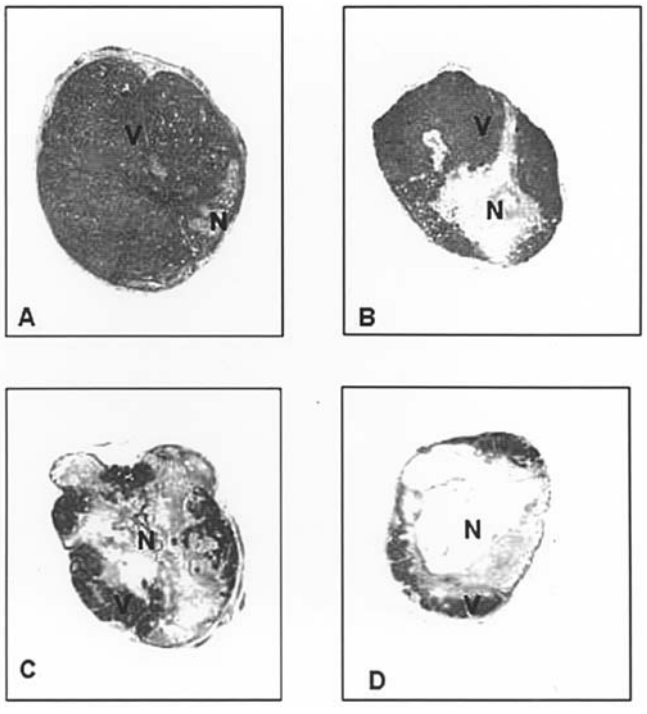


Figure 5. Effect of increasing doses of CA4-P on tumour necrosis in SW1222 colorectal tumour xenografts at 24-h post treatment. V, viable tissue; N, necrotic tissue. (A), Untreated; (B), 30 mg/kg CA-4-P; (C), 100 mg/kg CA-4-P; (D), 200 mg/kg CA-4-P.

$p<0.0001$) and at 24 h ($r=-0.48$, $p<0.05$), respectively. There were no significant changes in muscle (representative normal tissue) parameters at any time point or dose level (data not shown).

*Spatial heterogeneity of IAUGC response*. The baseline mean IAUGC values (pooled control groups) were rim: 0.079 mM.min; intermediate: 0.056 mM.min; centre: 0.050 mM.min (highly significant differences between each group by paired t-test). The percentage differences in IAUGC between each treatment group and the controls for each region are summarized in Fig. 3. For every dose and time, the order of change (reduction) in the group mean IAUGC was the same: centre > intermediate > rim. The ratio of centre: rim IAUGC was found to be significantly lower at 4 h after 100 and 200 mg/kg CA-4-P and at 24 h after 100 mg/kg CA-4-P than in the corresponding control groups.

*Effect of CA-4-P dose on functional vascular volume and tumor necrosis*. The reduction in functional vascular volume seen with CA-4-P was significant for all dose levels at 4 h and at 100 and 200 mg/kg at 24 h (Fig. 4A and B). The control tumors were mainly viable. Thirty mg/kg CA-4-P produced patchy hemorrhagic necrosis at 24 h whereas 100 mg/kg and 200 mg/kg produced extensive hemorrhagic necrosis with only a thin viable rim of tumor remaining (Fig. 5). Percentage necrosis was significantly different from control for all three doses and between 30 mg/kg and 100 mg/kg or 200 mg/kg but not between 100 mg/kg and 200 mg/kg (Fig. 4C).

*Effect of CA-4-P on $^{131}$I-A5B7 biodistribution*. Fig. 6 shows biodistribution of $^{131}$I-A5B7 (0.9 MBq/5.0 $\mu$g antibody) at 96 h in tumor and normal tissues, when given either as a single agent or combined with increasing doses of CA-4-P at 48 h. The antibody alone produced good tumor to normal tissue ratios (e.g. tumor:blood 2.8:1). Combining the antibody with 30, 100 or 200 mg/kg CA-4-P significantly increased its retention within the tumor by 70%, 78% and 89% respectively compared with antibody alone ($p<0.03$). Normal tissues remained unaffected ($p>0.5$). Tumor: blood ratios for the combination were 4:1, 4.5:1 and 4.5:1 respectively, as the dose of CA-4-P was increased. However, no significant difference was found between the amounts of antibody retained within the tumor for the 3 doses of CA-4-P ($p>0.5$).

## Discussion

There was a significant decrease in the IAUGC for Gd-DTPA in tumor (but not in muscle) following all three dose levels of CA-4-P, at 4 h after treatment. This persisted at the highest

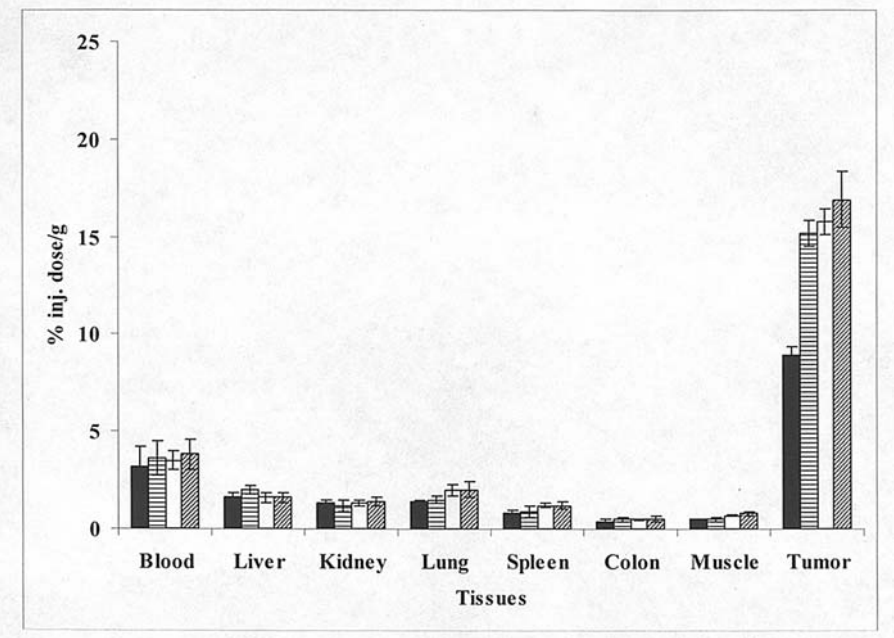


Figure 6. Ninety-six-hour biodistribution of $^{131}$I-labelled A5B7 (0.9 MBq/5.0 $\mu$g antibody) in nude mice given either no further treatment, or escalating doses of CA-4-P at 48 h. Left to right, antibody alone (black); antibody + 30 mg/kg CA-4-P (horizontal bars); antibody + 100 mg/kg CA-4-P (white); antibody + 200 mg/kg CA-4-P (diagonal bars). Bars are means of groups of 4 animals ± one standard error of the mean.

dose (200 mg/kg) for at least 24 h. The parameter $K^{trans}$ was a less sensitive indicator of CA-4-P effects, possibly because of assumptions made in the modeling procedure, including the use of a Gd-DTPA arterial input function. The arterial input function obtained in the present study does appear to be a good approximation based on: a) compatibility with previously published mouse arterial input function model parameters (40,45,46), b) generally good fitting of tumor and muscle data, and c) plausible values of $K^{trans}$ are obtained. However, this arterial input function was obtained from a separate group of mice and no corrections could be made for individual variability or any systemic CA-4-P effects. We note that a standardized model arterial input function will also be used for the proposed clinical studies (47).

The analysis of spatial heterogeneity of IAUGC values compared to distance from the edge of the tumor provides evidence that in this tumor model: a) blood flow is higher towards the tumor rim than in the centre of untreated tumors, and b) the magnitude of CA-4-P anti-vascular effects is higher in the tumor centre than in the rim. Although survival of cells in the periphery of tumors following treatment with CA-4-P and similar agents is a common finding, few studies have attempted to measure the early vascular effects in different tumor regions and results have been inconsistent (13,27,48). In the SW1222 tumor, there was clear peripheral sparing, in terms of both the initial vascular effects and the ultimate tumor cell necrosis. The reasons for this remain unclear but may relate to a larger vascular reserve in the periphery compared to the central region (as indicated by the respective pre-treatment IAUGC values).

The reduction in functional vascular volume seen in the SW1222 tumor following CA-4-P administration is similar to that seen in other tumors (11). The size and pattern of change in the MR parameters mirrors the changes seen in functional vascular volume and therefore provides evidence that using DCE-MRI with Gd-DTPA in clinical trials provides a reliable measure of tumor vascular response to CA-4-P.

It is assumed that a certain level of anti-vascular response to CA-4-P will be required for enhancement of RIT. The dose of CA-4-P used in the initial preclinical study of $^{131}$I-A5B7 and CA-4-P was 200 mg/kg (35). The dose with equivalent effectiveness in a human (expressed in mg/m$^2$) can be estimated either using a conversion (49) or by comparison of pharmacokinetic data [e.g. AUC for the active metabolite CA-4 (50)]. Whichever method is used, the equivalent human dose for 200 mg/kg in the mouse is approximately 10 times higher than the maximum tolerated dose in the phase I clinical trial of CA-4-P as a single agent (50). However, in the current study, it was found that the addition of CA-4-P at 48 h after antibody administration resulted in a similar increase in antibody retention over RIT alone at 96 h, for all CA-4-P doses (Fig. 6). Because the level of tumor necrosis created by the vascular disrupting agent (Fig. 4C) was significantly lower for 30 mg/kg (32.0%) than for 100 or 200 mg/kg (95.6% and 90.7% respectively), this suggests that the early response to CA-4-P was responsible for the enhanced antibody entrapment. Considering the marked dose response for the CA-4-P-induced vascular effects in the SW1222 tumor, it is quite surprising that 30 mg/kg CA-4-P was just as effective as 200 mg/kg in terms of antibody retention. It is possible that there was less difference in vascular efficacy between the doses during the first few hours after CA-4-P treatment and that the dose responses observed at 4 and 24 h reflect dose-related differences in vascular recovery rather than extent of initial shut-down. In any case, it appears that the vascular effect within the initial few hours after CA-4-P administration is critical for determining extent of antibody retention, at least when CA-4-P is given 48 h after the anti-

body. A second possibility is that, although blood flow resumes in the tumor periphery following temporary reduction or shut-down in response to CA-4-P, a significant number of vessels may be permanently lost in this region, ensuring antibody retention. Future work will investigate these and other possibilities.

An anti-vascular effect was seen most consistently at doses above 33 mg/m$^2$ of CA-4-P in phase I clinical trials [as measured by DCE-MRI or positron emission tomography (PET)) (28,31,32,50)]. Galbraith *et al* found that patients had mean reductions in tumor IAUGC and $K^{trans}$ of 33% and 37% respectively at 4 h following treatment with ≥52 mg/m$^2$ CA-4-P (31) - which are slightly lower than the reductions seen in the current study for 30 mg/kg CA-4-P at this time-point (38% and 57.5% respectively). This suggests that the 30 mg/kg dose level is similar to a clinically relevant human dose. The initial dose level of CA-4-P for the $^{131}$I-A5B7/ CA-4-P clinical trial is 50 mg/m$^2$.

In conclusion, there is a clear dose response relationship for treatment with CA-4-P, RIT and combined treatments in the SW1222 tumor. Significant reductions in kinetic parameters are seen at clinically relevant drug doses (30 mg/kg) and are of a similar magnitude to those seen in the previous clinical study (31). The data presented here indicate that although a 30 mg/kg dose of CA-4-P results in a substantially lower and shorter duration of anti-vascular effect than 100 and 200 mg/kg, there is no significant difference in radio-antibody retention between the 3 doses used, which is encouraging for the clinical trial of this approach.

## Acknowledgements

We would like to thank Professor Soren Bentzen for statistical advice, Ms. Gemma Lewis for technical help, and staff at the Gray Cancer Institute and The Royal Free and University College Medical School, for their care of the animals used in this study. This study was financially supported by the Cancer Research UK, Marie Curie Translational Research Trust, Cancer Treatment and Research Trust, National Translational Cancer Research Network, European Union FP6, LSHC-CT-2003-503233, STROMA.

## References

1. Napier M and Begent R: Radioimmunotherapy of gastrointestinal cancer. In: Cancer Radioimmunotherapy. Riva P (ed). Harwood Academia, Boston, MA, pp333-388, 1998.
2. Press OW, Eary JF, Appelbaum FR, *et al*: Radiolabeled-antibody therapy of B-cell lymphoma with autologous bone marrow support. N Engl J Med 329: 1219-1224, 1993.
3. Kaminski MS, Estes J, Zasadny KR, *et al*: Radioimmunotherapy with iodine ($^{131}$)I tositumomab for relapsed or refractory B-cell non-Hodgkin lymphoma: updated results and long-term follow-up of the University of Michigan experience. Blood 96: 1259-1266, 2000.
4. Goldenberg DM: Targeted therapy of cancer with radiolabeled antibodies. J Nucl Med 43: 693-713, 2002.
5. Jain RK and Baxter LT: Mechanisms of heterogeneous distribution of monoclonal antibodies and other macromolecules in tumors: significance of elevated interstitial pressure. Cancer Res 48: 7022-7032, 1988.
6. Jain RK: Delivery of novel therapeutic agents in tumors: physiological barriers and strategies. J Natl Cancer Inst 81: 570-576, 1989.
7. Pedley RB, El-Emir E, Flynn AA, *et al*: Synergy between vascular targeting agents and antibody-directed therapy. Int J Radiat Oncol Biol Phys 54: 1524-1531, 2002.
8. Flynn AA, Green AJ, Boxer GM, Casey JL, Pedley RB and Begent RH: A novel technique, using radioluminography, for the measurement of uniformity of radiolabelled antibody distribution in a colorectal cancer xenograft model. Int J Radiat Oncol Biol Phys 43: 183-189, 1999.
9. Boucher Y, Baxter LT and Jain RK: Interstitial pressure gradients in tissue-isolated and subcutaneous tumors: implications for therapy. Cancer Res 50: 4478-4484, 1990.
10. Dark GG, Hill SA, Prise VE, Tozer GM, Pettit GR and Chaplin DJ: Combretastatin A-4, an agent that displays potent and selective toxicity toward tumour vasculature. Cancer Res 57: 1829-1834, 1997.
11. Chaplin DJ, Pettit GR and Hill SA: Anti-vascular approaches to solid tumour therapy: evaluation of combretastatin A4 phosphate. Anticancer Res 19: 189-195, 1999.
12. Grosios K, Holwell SE, McGown AT, Pettit GR and Bibby MC: *In vivo* and *in vitro* evaluation of combretastatin A-4 and its sodium phosphate prodrug. Br J Cancer 81: 1318-1327, 1999.
13. Tozer GM, Prise VE, Wilson J, *et al*: Combretastatin A-4 phosphate as a tumor vascular-targeting agent: early effects in tumors and normal tissues. Cancer Res 59: 1626-1634, 1999.
14. Kanthou C and Tozer GM: The tumor vascular targeting agent combretastatin A-4-phosphate induces reorganization of the actin cytoskeleton and early membrane blebbing in human endothelial cells. Blood 99: 2060-2069, 2002.
15. Prise VE, Honess DJ, Stratford MR, Wilson J and Tozer GM: The vascular response of tumor and normal tissues in the rat to the vascular targeting agent, combretastatin A-4-phosphate, at clinically relevant doses. Int J Oncol 21: 717-726, 2002.
16. Bohle AS, Leuschner I, Kalthoff H and Henne-Bruns D: Combretastatin A-4 prodrug: a potent inhibitor of malignant hemangioendothelioma cell proliferation. Int J Cancer 87: 838-843, 2000.
17. Hill SA, Chaplin DJ, Lewis G and Tozer GM: Schedule dependence of combretastatin A4 phosphate in transplanted and spontaneous tumour models. Int J Cancer 102: 70-74, 2002.
18. Chaplin D and Hill S: The development of combretastatin A4 phosphate as a vascular targeting agent. Int J Radiat Oncol Biol Phys 54: 1491-1496, 2002.
19. Grosios K, Loadman PM, Swaine DJ, Pettit GR and Bibby MC: Combination chemotherapy with combretastatin A-4 phosphate and 5-fluorouracil in an experimental murine colon adenocarcinoma. Anticancer Res 20: 229-233, 2000.
20. Siemann DW, Mercer E, Lepler S and Rojiani AM: Vascular targeting agents enhance chemotherapeutic agent activities in solid tumor therapy. Int J Cancer 99: 1-6, 2002.
21. Li L, Rojiani A and Siemann D: Targeting the tumor vasculature with combretastatin A-4 disodium phosphate: effects on radiation therapy. Int J Radiat Oncol Biol Phys 42: 899-903, 1998.
22. Murata R, Siemann DW, Overgaard J and Horsman MR: Interaction between combretastatin A-4 disodium phosphate and radiation in murine tumors. Radiother Oncol 60: 155-161, 2001.
23. Horsman MR and Murata R: Combination of vascular targeting agents with thermal or radiation therapy. Int J Radiat Oncol Biol Phys 54: 1518-1523, 2002.
24. Beauregard DA, Thelwall PE, Chaplin DJ, Hill SA, Adams GE and Brindle KM: Magnetic resonance imaging and spectroscopy of combretastatin A4 prodrug-induced disruption of tumour perfusion and energetic status. Br J Cancer 77: 1761-1767, 1998.
25. Beauregard DA, Hill SA, Chaplin DJ and Brindle KM: The susceptibility of tumors to the antivascular drug combretastatin A4 phosphate correlates with vascular permeability. Cancer Res 61: 6811-6815, 2001.
26. Beauregard DA, Pedley RB, Hill SA and Brindle KM: Differential sensitivity of two adenocarcinoma xenografts to the anti-vascular drugs combretastatin A4 phosphate and 5,6-dimethylxanthenone-4-acetic acid, assessed using MRI and MRS. NMR Biomed 15: 99-105, 2002.
27. Maxwell R, Wilson J, Prise V, *et al*: Evaluation of the anti-vascular effects of combretastatin in rodent tumours by dynamic contrast enhanced MRI. NMR Biomed 15: 89-98, 2002.
28. Dowlati A, Robertson K, Cooney M, *et al*: A phase I pharmacokinetic and translational study of the novel vascular targeting agent combretastatin A-4 phosphate on a single-dose intravenous schedule in patients with advanced cancer. Cancer Res 62: 3408-3416, 2002.

29. Evelhoch JL, Lo Russo PM, He Z, *et al*: Magnetic resonance imaging measurements of the response of murine and human tumors to the vascular-targeting agent ZD6126. Clin Cancer Res 10: 3650-3657, 2004.
30. Robinson SP, McIntyre DJ, Checkley D, *et al*: Tumour dose response to the antivascular agent ZD6126 assessed by magnetic resonance imaging. Br J Cancer 88: 1592-1597, 2003.
31. Galbraith SM, Maxwell RJ, Lodge MA, *et al*: Combretastatin A4 phosphate has tumour anti-vascular activity in rat and man as demonstrated by dynamic magnetic resonance imaging. J Clin Oncol 21: 2831-2842, 2003.
32. Stevenson JP, Rosen M, Sun W, *et al*: Phase I trial of the antivascular agent combretastatin A4 phosphate on a 5-day schedule to patients with cancer: magnetic resonance imaging evidence for altered tumor blood flow. J Clin Oncol 21: 4428-4438, 2003.
33. Tofts PS and Kermode AG: Measurement of the blood-brain barrier permeability and leakage space using dynamic MR imaging. 1. Fundamental concepts. Magn Reson Med 17: 357-367, 1991.
34. Tofts PS: Modeling tracer kinetics in dynamic Gd-DTPA MR imaging. J Magn Reson Imaging 7: 91-101, 1997.
35. Pedley R, Hill S, Boxer G, *et al*: Eradication of colorectal xenografts by combined radioimmunotherapy and combretastatin A-4 3-O-phosphate. Cancer Res 61: 4716-4722, 2001.
36. Richman PI and Bodmer WF: Control of differentiation in human colorectal carcinoma cell lines: epithelial-mesenchymal interactions. J Pathol 156: 197-211, 1988.
37. Sharma SK, Pedley RB, Bhatia J, *et al*: Sustained tumor regression of human colorectal cancer xenografts using a multifunctional mannosylated fusion protein in antibody-directed enzyme prodrug therapy. Clin Cancer Res 11: 814-825, 2005.
38. Hittmair K, Gomiscek G, Langenberger K, Recht M, Imhof H and Kramer J: Method for the quantitative assessment of contrast agent uptake in dynamic contrast-enhanced MRI. Magn Reson Med 31: 567-571, 1994.
39. Donahue K, Burstein D, Manning W and Gray M: Studies of Gd-DTPA relaxivity and proton exchange rates in tissue. Magn Reson Med 32: 66-76, 1994.
40. Furman-Haran E, Margalit R, Grobgeld D and Degani H: Dynamic contrast-enhanced magnetic resonance imaging reveals stress-induced angiogenesis in MCF7 human breast tumors. Proc Natl Acad Sci USA 93: 6247-6251, 1996.
41. Evelhoch JL: Key factors in the acquisition of contrast kinetic data for oncology. J Magn Reson Imaging 10: 254-259, 1999.
42. Kety S: Blood-tissue exchange methods. Theory of blood-tissue exchange and its application to measurement of blood flow. Meth Med Res 8: 223-227, 1960.
43. Chalkley H: Method for the quantitative morphologic analysis of tissues. J Natl Cancer Inst 4: 47-53, 1943.
44. Smith KA, Hill SA, Begg AC and Denekamp J: Validation of the fluorescent dye Hoechst 33342 as a vascular space marker in tumours. Br J Cancer 57: 247-253, 1988.
45. Lyng H, Dahle GA, Kaalhus O, Skretting A and Rofstad EK: Measurement of perfusion rate in human melanoma xenografts by contrast-enhanced magnetic resonance imaging. Magn Reson Med 40: 89-98, 1998.
46. Checkley D, Tessier JJ, Kendrew J, Waterton JC and Wedge SR: Use of dynamic contrast-enhanced MRI to evaluate acute treatment with ZD6474, a VEGF signalling inhibitor, in PC-3 prostate tumours. Br J Cancer 89: 1889-1895, 2003.
47. Weinmann HJ, Laniado M and Mutzel W: Pharmacokinetics of GdDTPA/dimeglumine after intravenous injection into healthy volunteers. Physiol Chem Phys Med NMR 16: 167-172, 1984.
48. Maxwell R, Wilson J, Tozer G, Barber P and Vojnovic B: Segmentation of magnetic resonance images according to contrast agent uptake kinetics using a competitive neural network. In: Artificial Neural Networks in Medicine and Biology. Malmgren H, Borga M and Niklasson L (eds). Springer-Verlag, London, pp93-98, 2000.
49. Chodera A and Feller K: Some aspects of pharmacokinetic and biotransformation differences in humans and mammal animals. Int J Clin Pharmacol Biopharm 16: 357-360, 1978.
50. Rustin GJ, Galbraith SM, Anderson H, *et al*: Phase I clinical trial of weekly combretastatin A4 phosphate: clinical and pharmacokinetic results. J Clin Oncol 21: 2815-2822, 2003.